# PFTIR Test of Steam-Assisted Elevated Flares – Port Arthur

Final Report
June 17, 2011

Flint Hills Resources Port Arthur, LLC
Port Arthur Chemicals
4241 Savannah Avenue
Port Arthur, Texas 77640

Testing Conducted
October 21 – November 8, 2010

Prepared by
Clean Air Engineering, Inc.
Project No: 11085

# Table of Contents

## Appendix List

**Appendix A.1** – EPA 114 Request
**Appendix A.2** – Flare Specifications and Equipment
**Appendix A.3** – Calculations
**Appendix A.4** – PFTIR Description
**Appendix A.5** – PFTIR Theory and Operation
**Appendix A.6** – Video Camera Descriptions
**Appendix A.7** – Individual Test Series Results and Charts
**Appendix A.8** – Individual Test Series Process Conditions
**Appendix A.9 –** Individual Run Results Data Tables
**Appendix A.10** – Individual Run Vent Gas Composition Charts
**Appendix A.11** – Wind Data Tables
**Appendix A.12** – PFTIR QA/QC
**Appendix A.13** – Electronic Minute Data
**Appendix A.14** – Electronic PFTIR Raw Spectral Data
**Appendix A.15** – Video of Runs
**Appendix A.16** – Flare Visual Rating Data Sheets
**Appendix A.17** – Independent Source Test Calibration Data
**Appendix A.18** – Independent Source Test Gas Certifications
**Appendix A.19** – Laboratory Records for AU Sample Bags
**Appendix A.20** – Clock Synchronization Forms
**Appendix A.21** – Hydrogen Net Heating Value Adjustment

# 1.0 Overview

## 1.1 Introduction

As required by a Clean Air Act Section 114 request in Appendix A.1, Flint Hills Resources Port Arthur, LLC (FHR) conducted PFTIR testing of the Aromatics Unit (AU) and Light Olefins Unit (LOU) flares at their facility in Port Arthur, TX, in October and November of 2010. The main objective of the tests was to better understand the impacts of steam on the overall performance of each flare in terms of combustion efficiency (CE). Two additional operating parameters were also examined during this test program. The effect of hydrogen on combustion efficiency was studied on the AU flare. The effect of vent gas flow rate on combustion efficiency was studied on the LOU flare. The PFTIR tests were conducted using a Passive Fourier Transform Infrared Spectroscopy (PFTIR) instrument developed and operated by Industrial Monitor and Control Corporation (IMACC). This report contains the AU and LOU flare test results.

**Figure 1.1-1: AU Flare (left) and LOU Flare (right)**

The test was conducted with the assistance of both Clean Air Engineering, Inc. (CAE) and Industrial Monitoring and Controls Corporation (IMACC).

Clean Air Engineering, Inc.
500 W Wood St.
Palatine, IL 60067

IMACC
800 Paloma, Suite 100
Round Rock, TX 78645

## 1.2 Test Program Overview

### *1.2.1 Objectives*

The overall objectives of the test program were as follows:

1. Evaluate the impacts of combustion efficiency over a range of operating scenarios by changing both flare vent gas composition and steam rates.

2. Evaluate key operating parameters such as steam to vent gas ratio (S/VG) and Net Heating Value of the Combustion Zone ($NHV_{cz}$) as indicators that may assist in maintaining flare operation at high efficiency conditions during day-to-day operation.

### *1.2.2 Flare Components*

FHR Port Arthur has two flares: the Aromatics Unit (AU) flare and Light Olefins Unit (LOU) flare. Each flare has automatic steam control logic and equipment that is used during normal operation. This control system was used to set each flare at the required test conditions described in Section 1.2.3. Details of control and measurement equipment used for each flare are contained in Appendix A.2.

#### *1.2.2.1 AU Flare Description*

The AU flare is an elevated (120 ft.) steam-assisted flare. The current tip has a diameter of 20 inches and was installed in 1996. This tip was manufactured by Callidus and has two points of steam addition: center steam and ring steam. The center steam is injected in the vent gas stack prior to reaching the flare tip, and the ring steam is injected with nozzles around the flare tip rim. Appendix A.2 contains design specifications for the AU flare.

The AU flare serves as relief for the Aromatics Unit. The typical AU flare vent gas flow rate during normal operation is approximately 800 lb/hr, or less than 0.4% of the hydraulic capacity (approximately a 250:1 turndown factor). Base load includes flare header gas from the Aromatics Unit, seal purges from rotating equipment, sample station vents, and various process vents from process equipment. The flare was operated with a constant center steam of approximately 500 lb/hr and variable ring steam for the AU flare PFTIR test.

#### *1.2.2.2 LOU Flare Description*

The LOU flare is an elevated (370 ft.) steam-assisted flare. The current tip has a diameter of 78 inches (equivalent diameter of 54 inches – see Appendix A.2 for calculation) and was installed in June 2010. This tip was manufactured by Callidus and has two points of steam addition: center steam and lower steam. The center steam is injected in the vent gas stack prior to reaching the flare tip, and the lower steam is injected through internal tubes interspersed throughout the flare tip. Appendix A.2 contains design specifications for the LOU flare.

The LOU flare serves as relief for the Light Olefins Unit. The typical LOU flare vent gas flow rate during normal operation is approximately 3,000 lb/hr, or less than 0.3% of the hydraulic capacity (approximately a 333:1 turndown factor). Base load includes flare header gas from the Light Olefins Unit, seal purges from rotating equipment, sample station vents, and various process vents from process equipment. The flare was operated with a constant center steam of approximately 2,890 lb/hr and variable lower steam for the LOU flare PFTIR test.

### *1.2.3 Test Conditions*

PFTIR test series were performed on both AU and LOU flares at their base loads. For the AU flare, additional test series were performed to study the effects of hydrogen on steam operating envelopes. For the LOU flare, additional test series were performed to study the effects of increased vent gas flow on steam operating envelopes. Each test series is described in the below sections.

#### ***1.2.3.1 AU Test Conditions***

Four test series (A, B, C, and D) were conducted by setting a vent gas composition and vent gas flow rate. Within the test series, the steam flow was varied to achieve a range of steam to vent gas ratios on a mass basis (S/VG). The rationale for each test series is as follows:

AU-A To simulate normal base load with typical flow conditions for the flare. This test represented day-to-day operation. Vent gas flow was between 600 lb/hr and 1,100 lb/hr, with a best effort to maintain the flow between 700 lb/hr and 1,000 lb/hr.

AU-B To simulate a vent gas composition with low hydrogen content. This test added additional natural gas to the base load to bring the total flow up to between 1,750 lb/hr and 2,250 lb/hr. Hydrogen content in the vent gas was below 15% by volume.

AU-C To simulate a vent gas composition with medium hydrogen content. This test added additional natural gas and hydrogen to the base load to bring the total flow up to match the volumetric flow rate of AU-B. Hydrogen content in the vent gas was between 25% and 35% by volume.

AU-D To simulate a vent gas composition with high hydrogen content. This test added additional natural gas and hydrogen to the base load to bring the total flow up to match the volumetric flow rate of AU-B. Hydrogen content in the vent gas was between 40% and 50% by volume.

Because the AU flare vent gas header did not have a gas chromatograph installed, vent gas sample bags were collected twice for each run and analyzed by the on-site FHR laboratory for vent gas composition. The sample bag analysis was corrected to 0% oxygen for the final vent gas composition results.

#### *1.2.3.2 LOU Test Conditions*

Three test series (A, B, and C) were conducted by setting a vent gas flow rate. Within the test series, the steam flow was varied to achieve a range of steam to vent gas ratios (S/VG). The rationale for each test series is as follows:

LOU-A To simulate normal base load with typical flow conditions for the flare. This test represented day-to-day operation. Vent gas flow was between 2,500 lb/hr and 3,500 lb/hr.

LOU-B To simulate an increase in vent gas flow. This test added an additional 5,000 lb/hr of fuel gas to the base load. A best effort was made to maintain the hydrogen content of the vent gas so that it did not vary by more than 5% by volume (absolute) from LOU-A.

LOU-C To simulate a further increase in vent gas flow. This test added an additional 10,000 lb/hr of fuel gas to the base load. A best effort was made to maintain the hydrogen content of the vent gas so that it did not vary by more than 5% by volume (absolute) from LOU-A.

#### *1.2.3.3 Run Lengths and Replicates*

Each test series had several runs that were performed at set steam to vent gas ratios on a mass basis (S/VG). Each run was repeated at least once. If the absolute difference in on-site preliminary combustion efficiency results for the two replicates was more than 5% and the average combustion efficiency was greater than 85%, a third replicate run would be performed. Additionally, at least 15 valid data points (as determined by CleanAir and IMACC site personnel from on-site preliminary data) were required to constitute a valid run.

The length for all initial replicate runs at a given condition was 30 minutes. At the conclusion of the initial run, the data was divided into 10-minute segments and analyzed. If none of the segment average combustion efficiencies varied from the 30 minute average by more than 0.5% absolute, the run length for the second replicate could be shortened to 20 minutes.

The S/VG set point for each set of replicate runs was incremented from the minimum or API 521 recommended steam rate using whole number S/VG steps to the incipient snuff point. If the S/VG set point resulted in visible emissions, the run would be discontinued after three minutes of Method 22 visible emissions.

## 1.3 PFTIR Testing Description

The IMACC instrument used to determine gas composition of the flare plume for each test condition listed in Section 1.2.3 is the Passive Fourier Transform Infrared (PFTIR) analyzer. PFTIR analysis operates on the principle of spectral analysis of thermal radiation emitted by hot gases. Passive means that no “active” infrared light source is used. Instead, the hot gases of the flare are the infrared source. The spectrometer is a receiver only. This approach is possible because the infrared emission spectra of hot gases have the same patterns or “fingerprints” as their absorption spectra do. Consequently, observing a flare with an infrared instrument allows for identification and quantification of species through emission spectroscopy just as with absorption spectroscopy. A detailed description of the instrument and testing procedure are found in Appendix A.4.

### *1.3.1 PFTIR Locations*

Two PFTIR instruments were used for this test program. They were placed at approximately 90° from one another in order to ensure a good view of the flare plume regardless of wind direction.

For the AU flare tests, one PFTIR location was inside a portable SeaCan container by the fenceline monitoring building (“SeaCan location”), and the second location was in a trailer on Miller Farm road (“Trailer location 1”). The Trailer location equipment was controlled from the SeaCan location via fiber optic and Ethernet cables. This allowed both PFTIRs to collect data during a run for simultaneous readings. However, only some runs had simultaneous readings due to wind and calibration restrictions.

For the LOU flare tests, the PFTIR at the SeaCan location was used, and the Trailer location was moved to the opposite end of Miller Farm road (“Trailer location 2”). The two locations were not connected by cable, so only one location could be controlled at a time. Thus, simultaneous readings were not performed for the LOU flare test.

Figure 1.3-1 shows a map of the PFTIR locations in relation to the flare. The PFTIR at the trailer locations (serial number “H”) was mounted inside the rear of the trailer. The PFTIR at the SeaCan location (serial number “A”) was mounted on a tripod and placed at the road location. Appendix A.4 contains more detailed information about each location.

## Figure 1.3-1: Map of PFTIR Locations in Relation to AU and LOU Flares

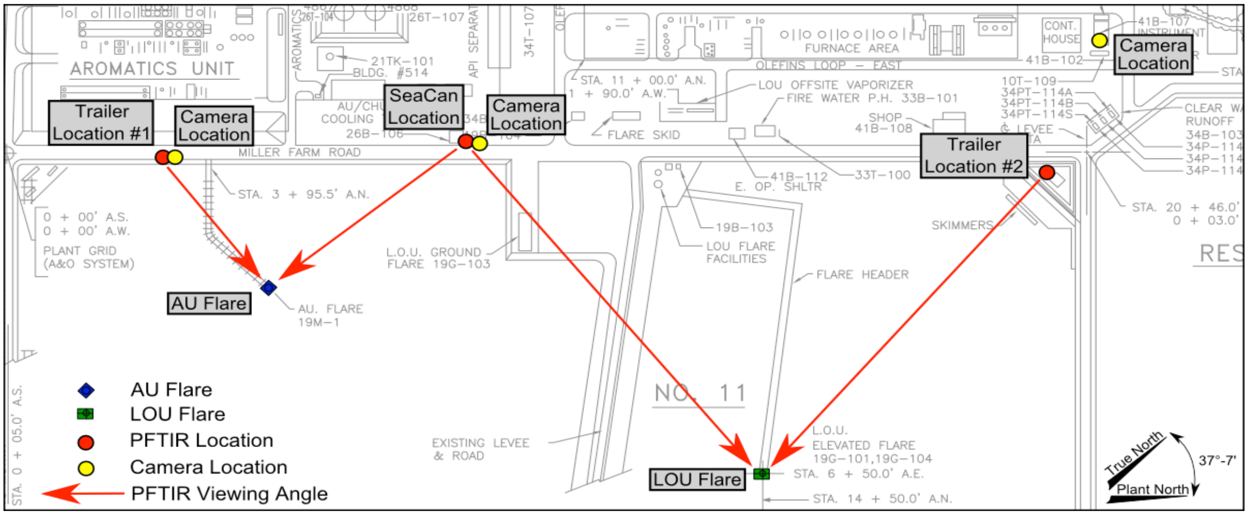

### *1.3.2 Video Recordings*

During the test program, video cameras recorded flare activity from the SeaCan and Trailer locations. At each location, one stationary visible light camera and one stationary infrared light camera were recording the flare tip. Additionally, one infrared camera was mounted on each PFTIR and recorded the aiming position of each PFTIR. For the Trailer location during the LOU test ("Trailer location 2"), the stationary visible and infrared cameras were located on the roof of the LOU control room. The types of cameras used during the test program are listed in Appendix A.6.

### *1.3.3 Preliminary Results and QA/QC*

On-site preliminary combustion efficiency results were computed. On-site replicate and run length decisions were made with the preliminary combustion efficiency results. By design, these preliminary results did not take into account the sky backgrounds, compound lists, and interferents that are incorporated after the test program is complete (see Appendix A.4). Thus, the final combustion efficiency results may change when all fraction are included in the analysis.

To ensure useable combustion efficiency results from the PFTIR, several QA/QC tests were performed during the test program. These tests included an independent source test, simultaneous measurements, and vertical traverses. Appendix A.12 contains data from these QA/QC tests.

### *1.3.4 Vertical Traverse*

In selecting an aiming point for the PFTIR near the center of the flare plume, an assumption is made that the combustion efficiency at this location is representative of the overall combustion efficiency of the flare. In order to test this assumption, a separate vertical traverse of the plume was conducted along with the LOU A 4.0 test series. Measurements were made at the top, the middle, and the bottom of the plume. This traverse was conducted under high wind conditions that would maximize the possibility of combustion efficiency stratification in the plume (i.e., higher combustion efficiency at the edges of the plume and lower combustion efficiency in the center.)

Details of the traverse are found in Appendix Section A.12.3. Figure 1.3-2 shows the results of the traverse. Note that regardless of whether the PFTIR measures at the top, the middle, or the bottom of the plume, the combustion efficiency is essentially constant.

## Figure 1.3-2: Vertical Traverse Results

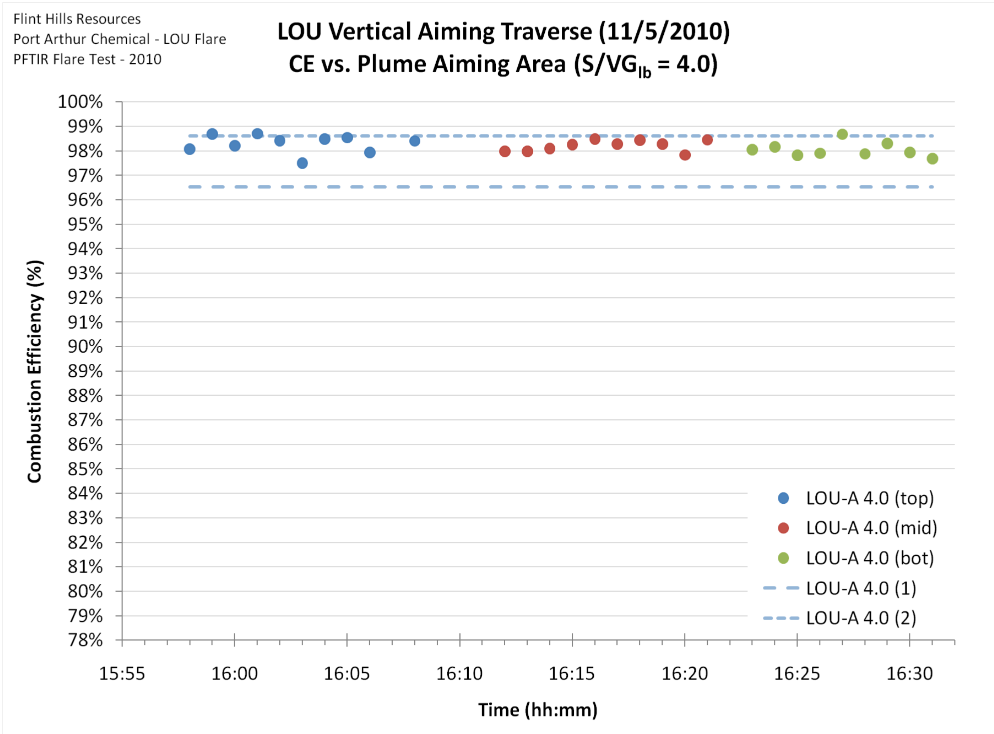

# 2.0 Results

For results presented in this section, relationships between combustion efficiency and three operating parameters were analyzed:

- **Visual Rating** – Flare flame visual emission readings (1-10 scale)
- **S/VG** – Actual steam to vent gas ratio (lb steam/lb vent gas)
- **$NHV_{cz}$** – Net heating value of the combustion zone (BTU/scf)

These parameters were selected because they can potentially be used during normal flare operation to maintain high combustion efficiency. Analysis of the combustion efficiency results from the PFTIR during this test established a relationship between combustion efficiency and these parameters. Descriptions of calculations for these parameters are contained in Appendix A.3. Appendix A.7 contains tables and charts of completed runs based on the requirements of the 114 Request. Appendices A.7 through A.11 also contain detailed condition and run information for each test.

## 2.1 Visual Rating

Visual ratings can be performed quickly and easily by flare operators without specialized equipment or instruments. Visual observations are an effective tool to be used in conjunction with the other operating parameters S/VG and $NHV_{cz}$. A relationship between combustion efficiency and visual rating may help an operator identify desirable flare operating conditions. However, this parameter is limited in that flare combustion efficiency is not easily determined when the flare flame is transparent.

Flare visual readings were collected during the test program using the scale established for the PFTIR test. Table 2.1-1 describes the flare visual rating scale.

The incipient smoke point is designated as the number 5 (the center of the scale), and represents the point at which the flare displays a “marbled” texture, indicative of small carbon soot particles forming in the combustion zone but quickly dissipating. No visible soot particles are present outside of the flame boundary at the incipient smoke point.

Flame ratings above 5 indicate increasing visible emissions extending beyond the flame boundary observed by an increasingly distinct trailing smoke plume. Flame ratings less than 5 indicate a visible flame decreasing in intensity until it becomes transparent. Ratings of 2 to 4 indicate a visible flame and a rating of 1 indicates a transparent flame. A flame rating of 0 indicates that the flare may be extinguished with steam visually present.

## Table 2.1-1: Flare Visual Rating Scale

| Flame Rating | Flame Characteristic |
|---|---|
| 0 | Steam plume |
| 1 | Transparent |
| 2 | Mostly transparent, with occasional yellow flame. |
| 3 | Mostly yellow flame, with occasional transparency. |
| 4 | Yellow to orange flame. |
| 5 | Orange flame with some dark areas in the flame. (Incipient smoke point) |
| 6 | Orange flame with light smoke trail. |
| 7 | Clear steam at the flare tip, with an orange flame and a light smoke trail. |
| 8 | Orange flame with dark smoke trail leaving the flame. |
| 9 | Orange flame with heavy dark smoke trail leaving the flame. |
| 10 | Billowing black smoke |

For the AU and LOU test programs, a FHR Port Arthur contractor recorded visual readings during each run using the flame rating scale. When the flare flame began consistently smoking (a rating of 6.0), the visual reader would alert the flare test control room and the run would be halted after 3 minutes of continuous visual emissions.

Figure 2.1-1 shows the relationship between combustion efficiency and visual rating for all runs in the AU flare tests. Most of the runs performed in the AU flare tests had transparent flames and low visual ratings.

Figure 2.1-2 shows the relationship between combustion efficiency and visual rating for all runs in the LOU flare tests. Like the AU flare tests, most of the runs performed in the LOU flare tests had transparent flames and low visual ratings.

## Figure 2.1-1: CE vs. Visual Rating for AU Flare Tests

# Figure 2.1-2: CE vs. Visual Rating for LOU Flare Tests

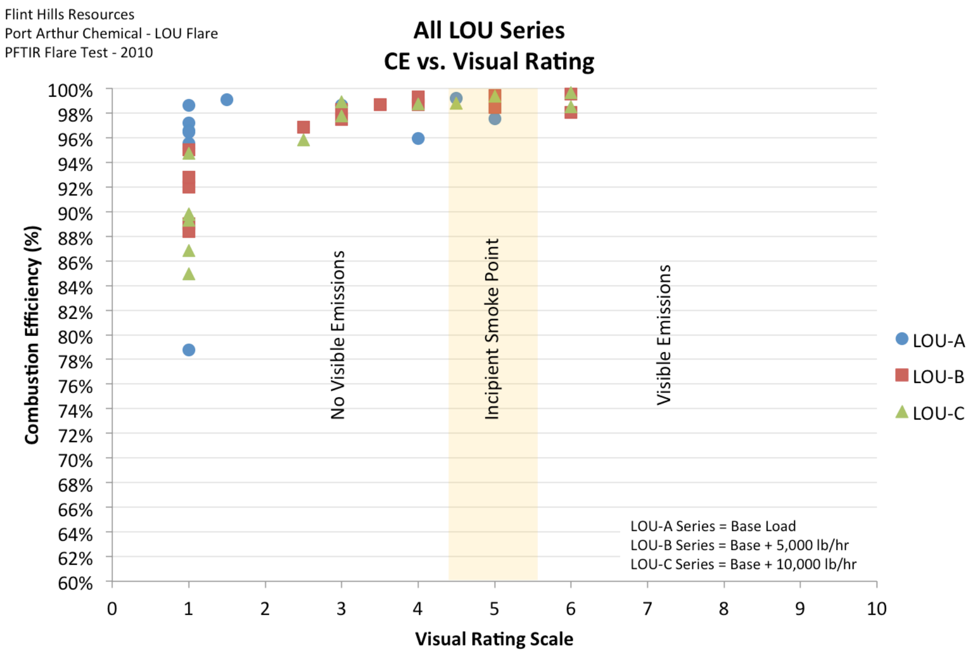

## 2.2 Steam to Vent Gas Ratio

S/VG can be used in control logic for maintaining smokeless combustion. Establishing a relationship between S/VG and combustion efficiency enables flare operators to better program steam control logic to improve combustion efficiency. However, S/VG alone may have limitations in its relationship to combustion efficiency. For example, a vent gas stream with high concentrations of inerts in the vent gas will not follow the same S/VG vs. combustion efficiency relationship as a vent gas stream with low concentrations of inerts.

PFTIR test runs for the AU and LOU flares were conducted at set steam to vent gas ratios (S/VG) on a mass basis (lb/lb). The S/VG set points for each run were established prior to the test by the 114 Request found in Appendix A.1. Figures showing S/VG ratios on a volumetric basis (scf/scf) are also included for comparison

For the AU flare base load (AU-A), low hydrogen (AU-B), mid hydrogen (AU-C), and high hydrogen (AU-D) test series, steam flow was increased from the point of incipient smoke to a point just before snuffing the flare (incipient snuff). For these test series, combustion efficiency remained relatively constant at a high level until the S/VG reached a point after which, combustion efficiency declined with increasing steam.

A mixture of hydrogen balanced with natural gas was added to the base load to achieve the desired hydrogen content (by volume) for the variable hydrogen tests. All of the variable hydrogen tests were performed at approximately the same volumetric flow rate. The vent gas for AU-B was less than 15% hydrogen content. The vent gas for AU-C had a hydrogen content between 25% and 35%. The vent gas for AU-D had hydrogen content between 40% and 50%. The increased hydrogen content appears to reduce the rate of combustion efficiency decline. Figure 2.2-1 shows this trend on a mass basis. Figure 2.2-3 shows this trend on a volumetric basis (scf/scf) for comparison.

For the LOU flare base load (LOU-A), mid flow (LOU-B), and high flow (LOU-C) series, steam flow was increased from the point of incipient smoke to a point just before snuffing the flare (incipient snuff). Like the AU flare results, combustion efficiency for the LOU flare remained relatively constant at a high level until the S/VG reached a point after which, combustion efficiency declined with increasing steam.

The LOU-B test series added an additional 5,000 lb/hr of fuel gas to the base load rate (3,000 lb/hr). Fuel gas was used because its hydrogen and methane content are similar to the LOU vent gas. The LOU-C test series added an additional 10,000 lb/hr of fuel gas to the base load rate. The rate of combustion efficiency decline seemed to increase slightly with increased vent gas flow. Figure 2.2-2 shows this trend on a mass basis. Figure 2.2-4 shows this trend on a volumetric basis (scf/scf) for comparison.

## Figure 2.2-1: Combustion Efficiency vs. S/VG (lb/lb): AU-A,B,C,D

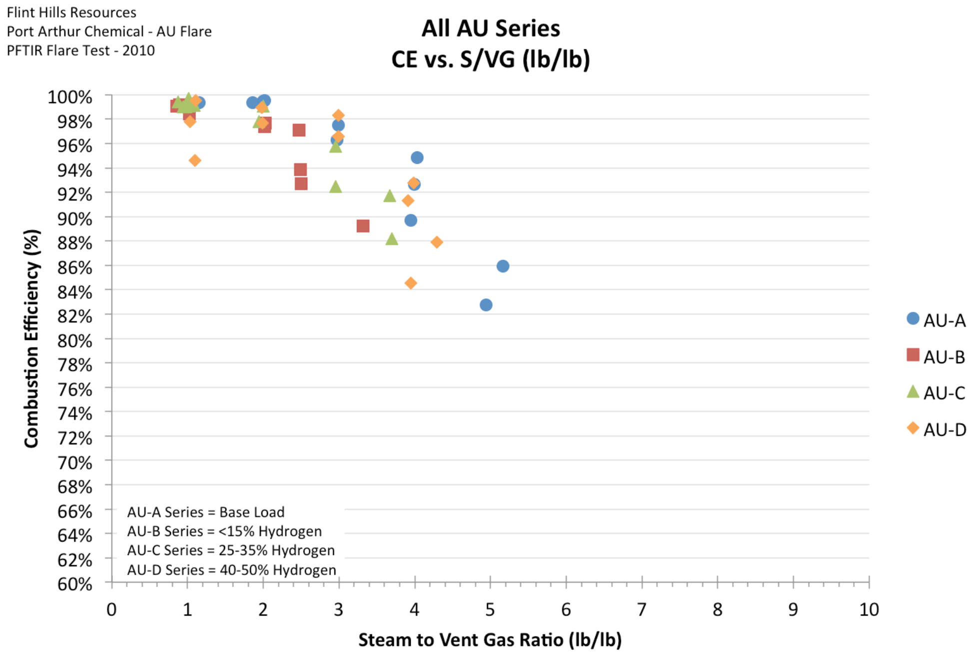


## Figure 2.2-2: Combustion Efficiency vs. S/VG (lb/lb): LOU-A,B,C

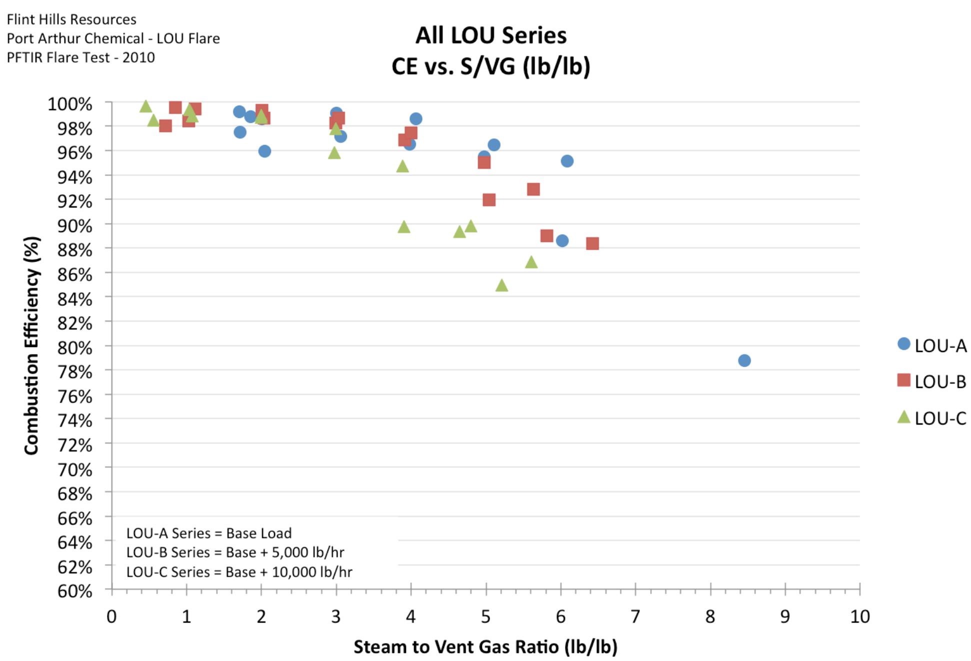

## Figure 2.2-3: Combustion Efficiency vs. S/VG (scf/scf): AU-A,B,C,D

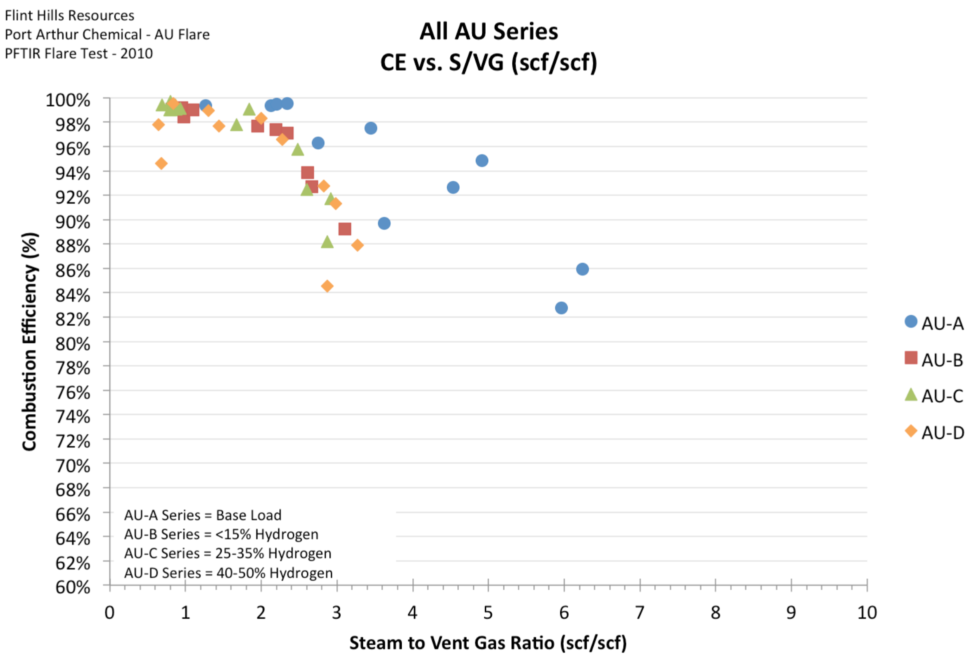


## Figure 2.2-4: Combustion Efficiency vs. S/VG (scf/scf): LOU-A,B,C

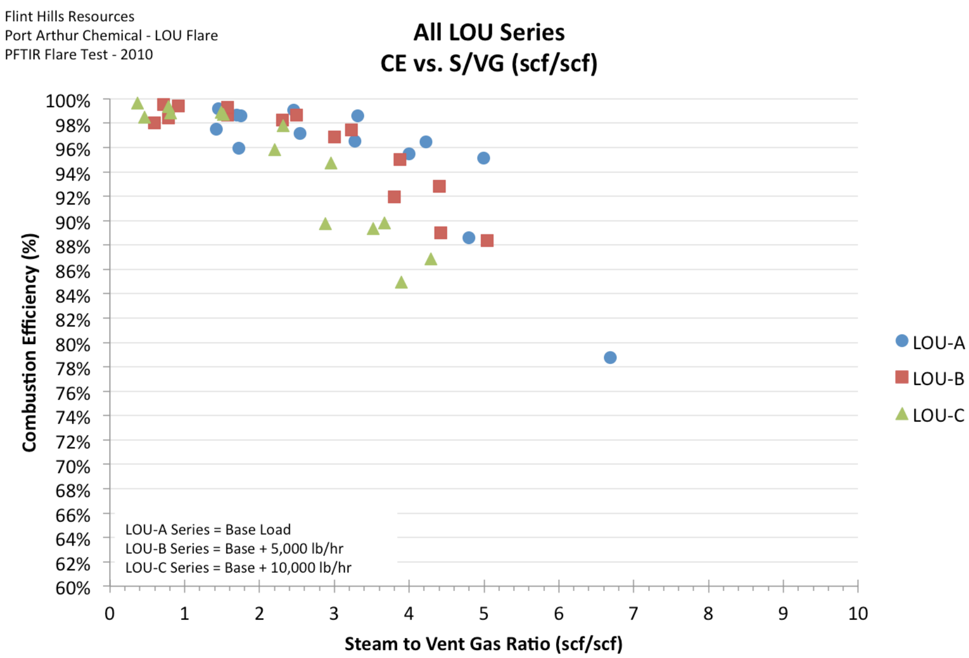

## 2.3 Net Heating Value of the Combustion Zone

$NHV_{cz}$ is another parameter that could be used to assist control of normal flare operation. The relationship between $NHV_{cz}$ and combustion efficiency has a wider scope and can take into account more process variables. For example, inerts in the vent gas are taken into account for the $NHV_{cz}$ calculation so the relationship to combustion efficiency remains valid when inerts are variable in the vent gas. However, $NHV_{cz}$ requires the flare operator to measure vent gas composition, which may require new equipment be installed on the vent header. Because the vent gas composition may only be measured in 10+ minute increments it also may be difficult to use $NHV_{cz}$ alone for control.

The Net Heating Value of the Combustion Zone ($NHV_{cz}$) , which includes total steam to the flare tip, is a calculated term representing the net heating value of all components in the combustion zone. The combustion zone is directly above the flare tip and is the point at which all materials combine for combustion. The $NHV_{cz}$ is therefore the resultant heat content from the mixture of the vent gas from the flare header, the pilot gas, and the total steam. To compensate for the observed effects of hydrogen, an adjusted $NHV_{cz}$ was calculated assuming hydrogen to have a net heating value of 1,212 BTU/scf instead of the unadjusted net heating value of 275 BTU/scf. For a more detailed discussion regarding the hydrogen adjusted $NHV_{cz,}$ calculation and value, see Appendix A.21.

Figure 2.3-1 shows the relationship between combustion efficiency and adjusted $NHV_{cz}$ for the AU flare tests.

Figure 2.3-2 shows the relationship between combustion efficiency and $NHV_{cz}$ for the LOU flare tests.

The adjusted $NHV_{cz}$ appears to compensate well for the effects of hydrogen on combustion efficiency decline. When a hydrogen net heating value of 1,212 BTU/scf is used, the adjusted $NHV_{cz}$ trends for the AU hydrogen test series (AU-B,C,D) shift into closer alignment. Figure 2.3-3 shows this shift from unadjusted $NHV_{cz}$ to adjusted $NHV_{cz}$ for the AU hydrogen tests.

The adjusted $NHV_{cz}$ does not compensate for the effects of vent gas flow rate on combustion efficiency decline. Figure 2.3-4 shows this shift from unadjusted $NHV_{cz}$ to adjusted $NHV_{cz}$ for the LOU tests.

## Figure 2.3-1: Combustion Efficiency vs. Adjusted $NHV_{cz}$: AU-A,B,C,D

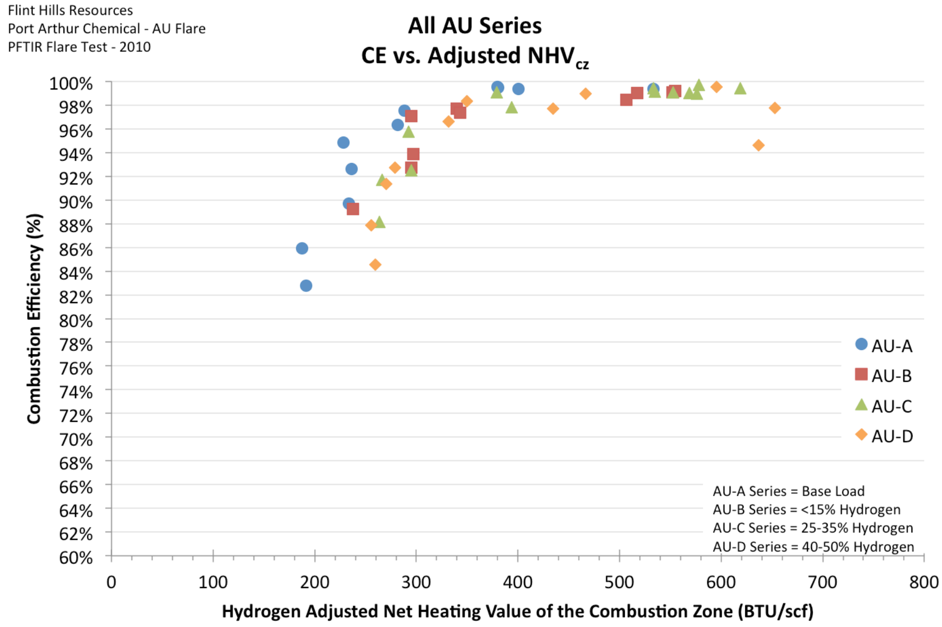


## Figure 2.3-2: Combustion Efficiency vs. Adjusted $NHV_{cz}$: LOU-A,B,C

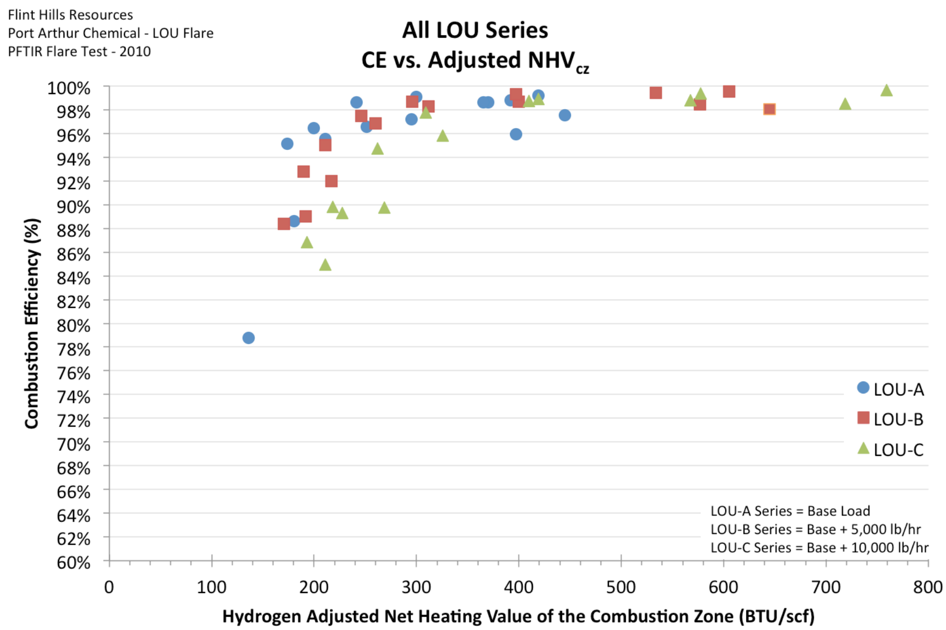

**Figure 2.3-3: Adjusted/Unadjusted $NHV_{cz}$ Comparison: AU-B,C,D**

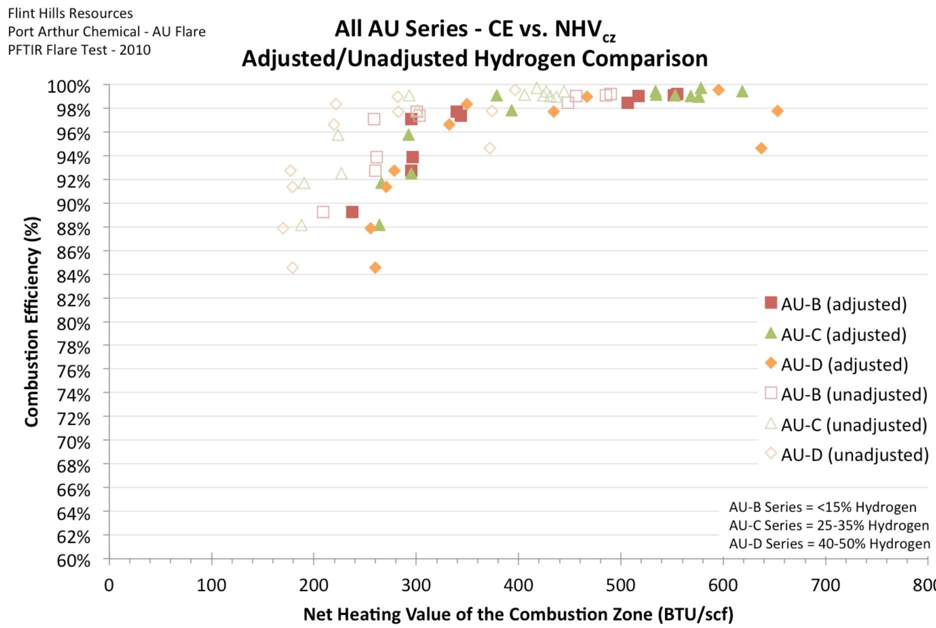


**Figure 2.3-4: Adjusted/Unadjusted $NHV_{cz}$ Comparison: LOU-A,B,C**

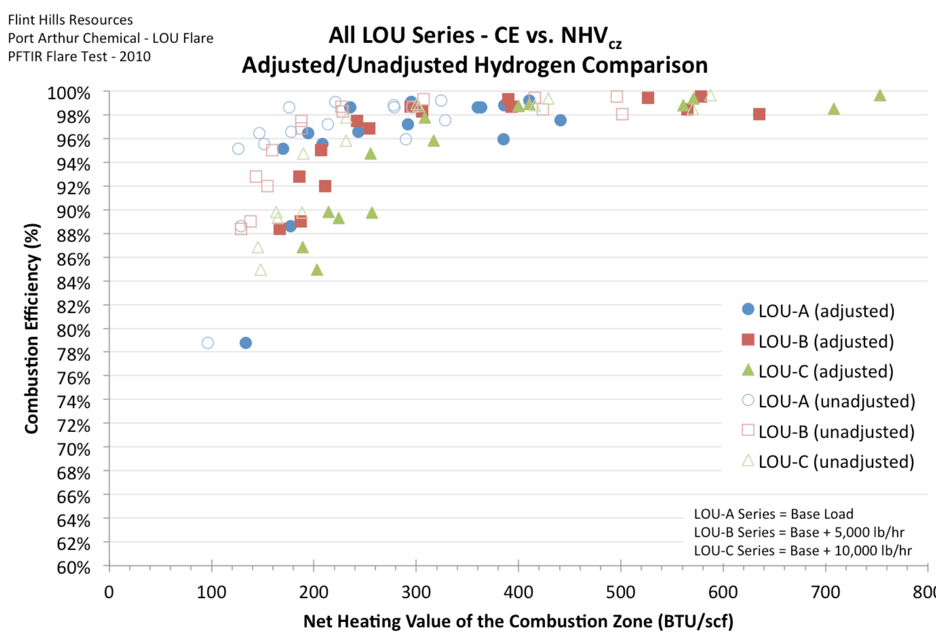

# 3.0 Conclusions

The PFTIR test of the AU and LOU flares at the FHR Port Arthur chemical plant provided data to support the following conclusions.

**Overall Observations**

General

- The data shows that both the AU and LOU flares exhibit a fairly broad high efficiency operating range that is consistent with current and past flare operating practices.
- Each of the three approaches to manage combustion efficiency (visibility, S/VG, and NHVcz) have advantages and disadvantages. Using a combination of these approaches will likely result in the most effective overall flare control strategy.

Visiblity

- Combustion efficiency generally begins to decline once the flame transitions from a smokeless, visible flame to one that is transparent. However, depending on the vent gas composition, not all transparent flames have poor combustion efficiency. This is most evident on the LOU flare results which contain a high hydrogen, high methane composition vent gas.
- A visible orange flame generally indicates good combustion efficiency.

S/VG

- Once adequate steam is supplied to prevent smoking, combustion efficiency generally declines with increased S/VG during normal and higher flow operations.
- Combustion efficiency will decline more rapidly with increased steam to vent gas ratios on a mass basis when the vent gas flow rate increases.

NHVcz

- The characteristics of hydrogen combustion are different than those of hydrocarbon combustion.
- Adjusting the net heating value of hydrogen from 275 BTU/scf to 1,212 BTU/scf more closely reflects the true combustion characteristics of hydrogen.
- Adjusting the net heating value of hydrogen brings the combustion efficiency trend lines into closer alignment when calculating the net heating value of the combustion zone.